Tricalcium Phosphate ($Ca_3(Po_4)_2$) With Dual Heterovalent Substitution for Obtaining Calcium-Phosphate Cements

Musoev Sharifdzhon Akhatovich[1]* and Knotko Alexander Valerevich[2]

[1]*Division of Interdisciplinary Materials Science, Faculty of Materials Science, Lomonosov Moscow State University, Russia*

[2]*Professor of the Faculty of Materials Sciences, Lomonosov Moscow State University (Russia, Moscow), Faculty of Chemistry, Russia*

*Corresponding author: Musoev Sharifdzhon Akhatovich, Division of Interdisciplinary Materials Science, Faculty of Materials Science, Lomonosov Moscow State University, Russian Federation, Russia

ARTICLE INFO

ABSTRACT

In this paper, cases of simultaneous replacement of Ca^{2+} by N^{a+} and PO_4^{3-} by SO_4^{2-} are considered. Solid solutions were synthesized by the solid-phase reaction $(1-x) \cdot Ca_3(PO_4)_2 + x \cdot (CaSO_4 + Na_2SO_4)$, where x=0.05; 0.15; 0.25. The synthesized samples were studied by X-ray diffraction and SEM with X-ray spectral microanalysis (XSMA), also the pH of the aqueous phase in contact with the substituted phosphates was measured. The XRD results showed that after substitution, the samples had a $Ca_3(PO_4)_2$ phase with a partial phase of Na_2SO_4 and after mixing with phosphoric acid, were obtained mixtures of brushite, monetite and TCP phases. According to the pH measurements of aqueous solutions of β-TCP substituted cements, the values of the medium ranged from 10 to 6.8, which indicates the possible further study of these samples for biological testing and the use of these materials for medicine.

Introduction

Bioresorbable bone implants are innovative medical materials that are used to replace or restore damaged or missing bone tissue. Such implants are made of a biocompatible material that decomposes over time and is replaced by the new bone tissue [1,2]. The advantage of bioresorbable bone implants is that they do not require secondary operations for removal, as they are naturally resorbed in the body. This reduces the risk of complications and shortens the patient's recovery time [3,4]. Besides that, implants should have high strength and stability, which allows them to maintain the structure and function of bone tissue for a long time. They provide optimal conditions for natural bone growth and regeneration [5,6]. Bioresorbable bone implants, based on phosphates, have emerged as a groundbreaking solution in the field of bone tissue restoration. One of the primary ad-

vantages of bioresorbable bone implants is their convenience. Unlike traditional implants, which require subsequent surgical removal after the bone has healed, bioresorbable implants eliminate the need for a second surgery. This not only reduces patient discomfort but also lowers the risk of complications associated with implant removal procedures [7,8].

Furthermore, biocements used in bone regeneration are composed of biocompatible materials that are well-tolerated by the body. This significantly reduces the likelihood of adverse reactions or complications, making biocements a safer option for patients. The other way of use of biocements is that they have compatibility with medical imaging techniques. Traditional metallic implants can interfere with imaging procedures such as X-rays, CT scans, and MRI scans, making it difficult to assess the progress of bone healing. Bioresorbable im-

plants are typically made from materials that are transparent to medical imaging techniques. This ensures that physicians can accurately monitor the healing process and make informed decisions regarding patient care without any hindrance [9,10]. As mentioned, bioresorbable bone implants are based on phosphates, and phosphates play a crucial role in bone tissue as they are essential components of hydroxyapatite, the mineral that gives bones their strength and rigidity [11,12]. Phosphates, particularly tricalcium phosphate (TCP), have been extensively studied and used for last decades in bone tissue engineering and regeneration.

TCP is a biocompatible material that closely resembles the mineral composition of natural bone. It is osteoconductive, meaning it provides a scaffold for new bone formation [13]. When TCP is implanted into a bone defect, it acts as a template for the deposition of new bone tissue. Over time, the TCP gradually resorbs and is replaced by newly formed bone. It supports the attachment, migration, and proliferation of osteoblasts, the cells responsible for bone formation. This enables the regeneration of damaged or lost bone tissue. TCP has the ability to stimulate the natural healing process in the body [14,15]. It releases calcium and phosphate ions, which are essential for bone mineralization.
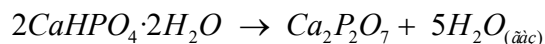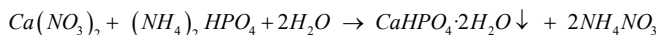
These ions promote the deposition of hydroxyapatite, a key component of natural bone. This not only enhances bone regeneration but also improves the mechanical properties of the newly formed tissue. However, despite all the advantages, tricalcium phosphate (TCP) has a relatively high speed of bioresorbability at which the material can prematurely break down and absorbed by the body. Its resorption rate can be controlled by adjusting the composition and porosity of the material [16,17]. Based on the foregoing, the aim of the work is to develop approaches to controlling the composition and microstructure of brushite calcium-phosphate cements through double heterovalent substitution.

Materials

Synthesized $Ca_2P_2O_7$, β-$Ca_3(PO_4)_2$, $CaCO_3$ (HIMMED, OSCh 16-2), commercial $CaSO_4$, Na_2SO_4, 3 M H_3PO_4 (GOST 6552-80 /IZM 1-2/).

Methods

To obtain tricalcium phosphate, calcium pyrophosphate $Ca_2P_2O_7$ was preliminarily synthesized by thermolysis of brushite $CaHPO_4\cdot2H_2O$, which was obtained by precipitation from an aqueous medium, described, for example, in the work [18]:

$$Ca(NO_3)_2 + (NH_4)_2HPO_4 + 2H_2O \rightarrow CaHPO_4\cdot2H_2O\downarrow + 2NH_4NO_3$$

$$2CaHPO_4\cdot2H_2O \rightarrow Ca_2P_2O_7 + 5H_2O_{(ãàç)}$$

Tricalcium phosphate was synthesized by the solid phase method according to the equation [18]:

$$CaCO_3 + Ca_2P_2O_7 = Ca_3(PO_4)_2 + CO_2\uparrow$$
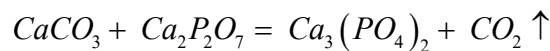
This reaction involves the decomposition of calcium carbonate and the formation of tricalcium phosphate. Stoichiometric weighed portions of the initial powders of calcium pyrophosphate and calcium carbonate were ground in a mortar. For more efficient grinding and mixing of reagents, grinding was carried out using hexane as a liquid medium. After that, the mixture was left in air for 10 minutes to evaporate the hexane. Then, the mixture of powders was poured into an alundum crucible, heated to 1100 ℃, and annealed at this temperature for 8 hours in a Nabertherm muffle furnace.

The $Ca_3(PO_4)_2$ samples with double heterovalent substitution were synthesized according to the following reaction scheme:

$$(1-x)Ca_3(PO_4)_2 + x(CaSO_4 + Na_2SO_4) = Ca_{3-2x}Na_{2x}(PO_4)_{2-2x}(SO_4)_{2x},$$
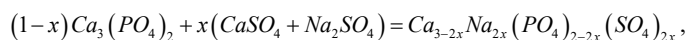
To carry out this reaction, the required amounts (x=0,05; 0,15; 0,25) of tricalcium phosphate, calcium sulfate and sodium sulfate were calculated. After weighing the corresponding amounts of the initial powders, they were ground in a mortar and annealed at a temperature of 950 ℃ for 8 hours.

In order to obtain brushite cements, the synthesized powders were mixed with 3 M H_3PO_4:

$$(Ca,Na)_3(PO4,SO_4)_2 + H_3PO_4 + 6H_2O => 3(Ca,Na)(HPO_4,SO_4)*2H_2O$$
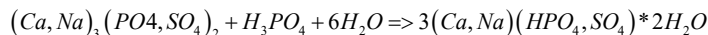
Characterization

The X-ray diffraction (XRD) analysis was conducted using a Rigaku D/Max-2500(Rigaku, Tokyo, Japan). The microstructure of the ceramic materials was studied using a LEO SUPRA 50VP (Carl Zeiss, Oberkochen, Germany) scanning electron microscope (SEM) with an acceleration voltage of 21 kV in low vacuum (40 Pa N2) regime. The images were recorded using low vacuum Everhart-Thornley secondary electron detector. The diffractograms were processed using the WinXpow software (version 1.2). The phase ratio in the samples was calculated using the corundum number method, and the size of the coherent scattering region was determined by the Scherrer's Equation:

$$d(CSR) = \frac{0.9\lambda_{Cu}}{\beta \cdot \cos\Theta}$$

where:

d(CSR) - is the mean size of the ordered (crystalline) domains;

λCu-is the X-ray wavelength;

β- is the line broadening at half the maximum intensity (FWHM), after subtracting the instrumental line broadening, in 2θ scale, radians.

θ- is the Bragg angle.

pH Measurements

The study of ion activity in solutions (pH) was carried out using a multichannel ion meter Econix-Expert-001 (Russia) equipped with a glass electrode. Calibration of the electrodes was conducted using solutions with known concentrations of the ions and standard buffer solutions with a given pH.

Results and Discussion

To study $Ca_{3-2x}Na_{2x}(PO_4)_{2-2x}(SO_4)_{2x}$ solid solutions, samples were obtained with molar ratios of the indicated components 0,75:0,25; 0,85:0,15; 0,95:0,05. The solid solution diffraction pattern is shown in (Figure 1). As can be seen from the figure, the 0.95:0.05 sample is single-phase, while the 0,75:0,25 and 0,85:0,15 samples are two-phase.

With partial replacement of the Ca^{2+} cation by Na^{+} and the PO_4^{3-} anion by SO_4^{2-}, the solid solution phase based on tricalcium phosphate remains the only one observed in the 0,95:0,05 sample. As the amount of sulfates in the samples 0,85:0,15 and 0,75:0,25 increases, we can observe the Na_2SO_4 phase, and the ratio between them (substituted TCP- Na_2SO_4) corresponds to 93:7% and 90:10%, respectively. The calculated sizes of coherent scattering regions for these samples are shown in (Table 1).

Table 1: Dimensions of coherent scattering regions for samples 0,95:0,05; 0,85:0,15; 0,75:0,25.

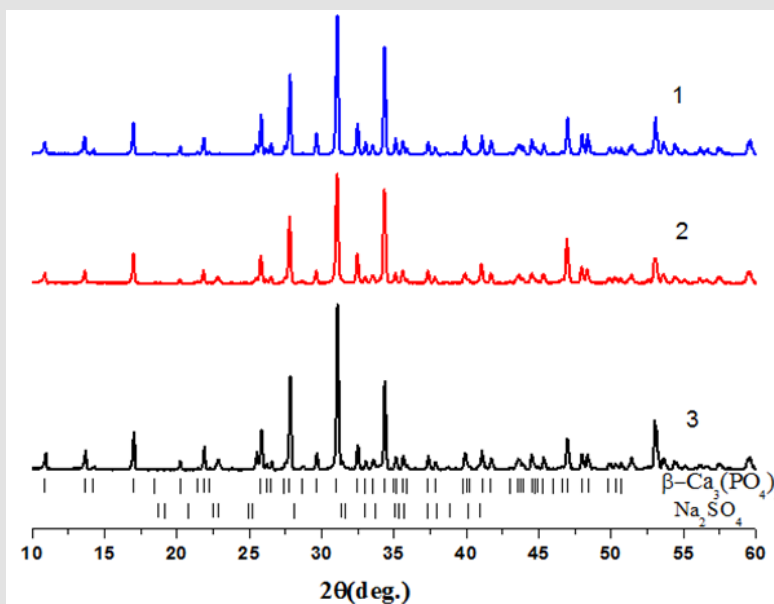| Coherent scattering region	0,95:0,05	0,85:0,15	0,75:0,25
d, nm	47,9	43,5	53,2

Figure 1: XRD results of the samples:
1)   0,95:0,05,
2)   0,85:0,15,
3)   0,75:0,25.

Brushite cements were obtained by mixing 3 M H_3PO_4 with a stoichiometric ratio of substituted TCP; the results of the phase analysis of the obtained cements are shown in (Figure 2). According to X-ray phase analysis, it can be said that in the case of TCP-0,95, the phases of brushite, monetite and TCP (mainly) are formed. With a ratio of TCP-0,85 and 0,75, both the brushite phase and the monetite phase are formed and part of the TCP (45%, 3%) remains in the samples TCP-0,85, TCP-0,75. Based on these data, it can be concluded that with an increase in the mole fraction of sulfates by more than 0,15, the TCP may, in this case, almost fully react with the acid.

Based on the diffraction pattern (Figure 2), the ratio of brushite, monetite, and TCP phases were calculated (using corundum numbers) and also the coherent scattering regions (CSR) were determined for the obtained brushite cements, which are shown in (Table 2). Based on the obtained data, it is possible to propose that when the ratio of TCP in the samples decreases, the brushite phase, on the contrary, increases, while the monetite phase remains almost unchanged. Thus, the content of more $CaSO_4$ and Na_2SO_4 in the samples encourages TCP to react with acid until the reaction is complete. Calculations of the sizes of the coherent scattering regions showed that, regardless of the change in the composition of the phases of the final samples, they remain approximately the same.
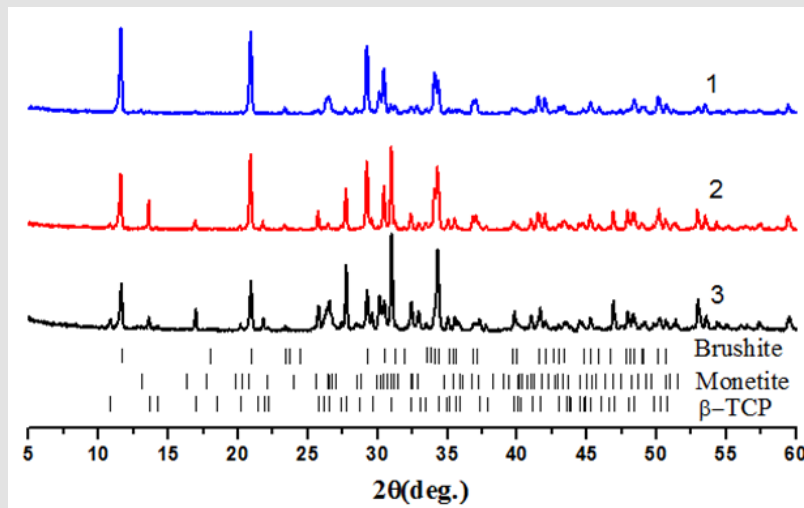
Figure 2: XRD for the obtained brushite cements from substituted TCP:
1) 0,75:0,25,
2) 0,85:0,15,
3) 0,95:0,05.

Table 2: Coherent scattering estimation sizes and phase ratio for the samples 0,95:0,05; 0,85:0,15; 0,75:0,25.

Mole fractions of samples	0,95:0,05			0,85:0,15			0,75:0,25		
phases	brushite	monetite	TCP	brushite	monetite	TCP	brushite	monetite	TCP
d, nm	45	17	57	50	42	55	44	21	58
Phase ratios, %	21	20	59	44	11	45	74	23	3

According to the microstructural analysis of the surface of the samples (Figure 3), it can be said that when $CaSO_4$ + Na_2SO_4 is added simultaneously, the individual morphology of all samples is lost, while in [19], for each substituted Na+, K+ cation and SiO_4^{4-} anion, SO_4^{2-} with β and α -TCP microparticles of their characteristic shape were obtained. On fig. (Figure 3) shows micrographs of the surface of the synthesized cement samples using β –TCP with double cationic and anionic substitution, which show the formation after acid mixing, flat and acicular micron-sized particles on the surface. It can be seen from the images that with an increase in the amount of sulfates in the samples, the particles begin to form a shape (plates) and become larger.
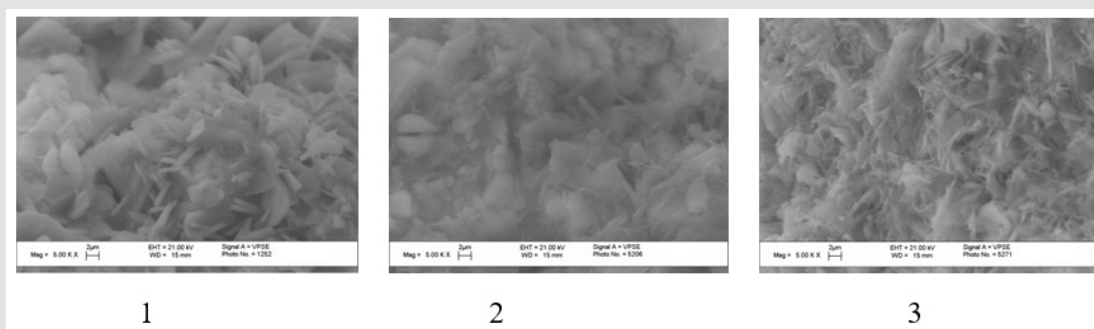

Figure 3: SEM images of the surface morphology of synthesized cements from substituted TCP:
1) 0,75:0,25,
2) 0,85:0,15,
3) 0,95:0,05.

For all obtained substituted TCP samples, pH measurements of the aqueous phase in contact with the phosphate material (1 g dry mix in 40 ml H_2O) were carried out. The measurements were carried out for 16 days, and showed that the pH values of the liquid (aqueous) phase do not go into the acidic or alkaline range (Figure 4), although at the initial stage (immediately after adding water), an increase in pH to 10 was recorded, followed by a decrease to values of about 7. This change may be associated with successive leaching of various compounds from the solid solution based on TCP.
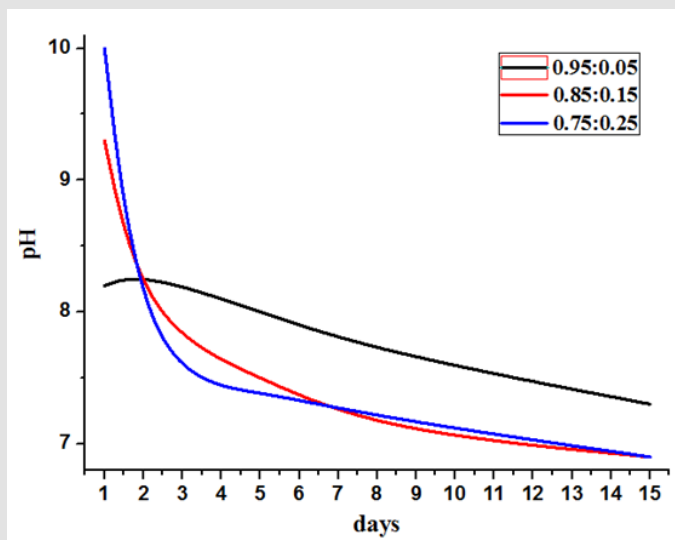

Figure 4: Time dependence of pH of water in contact with substituted TCP.

To confirm this assumption, the atomic ratios in the samples substituted with TCP before and after prolonged contact with water, were studied by the XSMA method (Table 3). As a result of this study, it was shown that for a sample of the TCP ratio of 0,95:0,05, there is a slight decrease in the Ca/Na ratio, and for other samples, this ratio noticeably increases after pH measurements, the P/S ratio practically does not change for the sample TCP 0,95:0,05 and slightly increases for the rest of the samples, the ratio (Ca + Na) / (P + S) for all samples slightly decreases. The observed changes correlate satisfactorily with the pH measurement data.

Table 3: Atomic fractions of elements before and after ionometry.

($CaSO_4$ + Na_2SO_4)	Ca/Na	P/S	(Ca+Na)/(P+S)
x=0,05	48,4	29,44	1.62
after pH	40,81	29,69	1.55
x=0,15	7,91	5,57	1.6
after pH	21,23	11,23	1.56
x=0,75	17,58	10,82	1.61
after pH	20,74	12,54	1.52

Conclusions

The XRD results showed that with an increase in the content of sulfates in samples of substituted TCP, the presence of the Na_2SO_4 phase is observed and a decrease in the amount of TCP in cement samples, when mixed with acid, mainly leads to the formation of a brushite phase. According to the phase ratios, it was found that the 0,75:0,25 sample contained the brushite phase, and the 0,95:0,05 sample contained the TCP phase as the main one. The sizes of the coherent scattering regions remained approximately the same regardless of the change in the final phases of the samples. The hydrolysis of the studied samples of substituted TCP was accompanied by the release of sulfate and sodium ions into the aqueous solution, which increased as their content in the solid solution increased. After holding in contact with water for two weeks, for solid solutions, the acidity of the medium turned out to be close to neutral. Microstructural analysis showed that after mixing with acid, flat, needle-shaped micron particles are formed and with an increase in the amount of sulfates in the samples, the particles begin to form a shape (plates) and become larger.

References

1. Al Shalawi F D, Mohamed Ariff A H, Jung D W, Mohd Ariffin M K A, Seng Kim C L, et al. (2023) Biomaterials as Implants in the Orthopedic Field for Regenerative Medicine: Metal versus Synthetic Polymers. Polymers 15(12): 2601.

2. Sheikh Z, Najeeb S, Khurshid Z, Verma V, Rashid H, et al. (2015) Biodegradable Materials for Bone Repair and Tissue Engineering Applications. Materials (Basel) 8(9): 5744-5794.

3. Claes L, Ignatius A (2002) Entwicklungneuer biodegradabler Implantate [Development of new, biodegradable implants]. Chirurg 73(10): 990-996.

4. Jia Li Wang, Jian Kun Xu, Chelsea Hopkins, Dick Ho Kiu Chow, Ling Qin (2020) Biodegradable Magnesium-Based Implants in Orthopedics—A General Review and Perspectives. Advanced Science 7(8): 1902443.

5. Amini AR, Laurencin CT, Nukavarapu SP (2012) Bone tissue engineering: recent advances and challenges. Crit Rev Biomed Eng 40(5): 363-408.

6. Tiffany Kim, Carmine Wang See, Xiaochun Li, DonghuiZhu (2020) Orthopedic implants and devices for bone fractures and defects: Past, present and perspective, Engineered Regeneration 1: 6-18,

7. Kretlow, James Mikos, Antonios (2007) Review: Mineralization of Synthetic Polymer Scaffolds for Bone Tissue Engineering. Tissue engineering 13(5): 927-938.

8. Pei Wang, Yan Gong, Guangdong Zhou, Wenjie Ren, Xiansong Wang (2023) Biodegradable Implants for Internal Fixation of Fractures and Accelerated Bone Regeneration. ACS Omega Article ASAP 8(31): 27920-27931.

9. Prakasam M, Locs J, Salma Ancane K, Loca D, Largeteau A, et al. (2017) Biodegradable Materials and Metallic Implants-A Review. J FunctBiomater 8(4): 44.

10. Hosseini ES, Dervin S, Ganguly P, Dahiya R (2021) Biodegradable Materials for Sustainable Health Monitoring Devices. ACS Appl Bio Mater 4(1): 163-194.

11. Nuss KM, von Rechenberg B (2008) Biocompatibility issues with modern implants in bone - a review for clinical orthopedics. OpenOrthop J 2: 66-78.

12. Hou X, Zhang L, Zhou Z, Luo X, Wang T, et al. (2022) Calcium Phosphate-Based Biomaterials for Bone Repair. J Funct Biomater 13(4): 187.

13. Polo Corrales L, Latorre Esteves M, Ramirez Vick JE (2014) Scaffold design for bone regeneration. J Nanosci Nanotechnol 14(1): 15-56.

14. Handschel Jörg, Wiesmann Hans, Stratmann Udo, Kleinheinz Johannes, Ulrich Meyer, et al. (2002) TCP is hardly resorbed and not osteoconductive in a non-loading calvarial model. Biomaterials 23(7): 1689-1695.

15. Negishi Koga T, Takayanagi H (2012) Bone cell communication factors and Semaphorins. Bonekey Rep 1: 183.

16. LeGeros RZ, LeGeros JP, Daculsi G, Kijkowska R, Wise DL, et al. (1995) Calcium-phosphate biomaterials: preparation, properties, and biodegradation. In: editors. Encyclopaedia Hand book of Biomaterials and Bioengineering. Part A, New York: Marcel Dekker 2(43): 1429-1463.

17. Fernandez deGrado G, Keller L, Idoux Gillet Y, Wagner Q, Musset AM, et al. (2018) Bone substitutes: a review of their characteristics, clinical use, and perspectives for large bone defects management. J Tissue Eng 9: 2041731418776819.

18. Сафронова Т В., Путляев В И. Медицинское неорганическое материаловедение в России: кальцийфосфатные материалы // Наносистемы: физика, химия, математика (2013) №1. URL: https://cyberleninka.ru/article/n/meditsinskoe-neorganicheskoe-materialovedenie-v-rossii-kaltsiyfosfatnye-materialy (date of the application: 05.08.2023).

19. Мусоев Ш А, Кнотько А В, Влияние изоморфных замещений в трикальцийфосфате $Ca_3(PO_4)2$ на микроструктурные и химические свойства получаемых из него фосфатных цементов // Неорганические материалы. — 2023. — Т. 59, № 4. — С. 399–407.

Submission Link: https://biomedres.us/submit-manuscript.php

Assets of Publishing with us

- Global archiving of articles
- Imm*e*diate, unrestricted online access
- Rigorous Peer Review Process
- Authors Retain Copyrights
- Unique DOI for all articles

https://biomedres.us/